Available online at www.CivileJournal.org

Civil Engineering Journal

(E-ISSN: 2476-3055; ISSN: 2676-6957)

Vol. 11, No. 06, June, 2025

Mechanical Characteristics of Prestressed Concrete Cylinder Pipe Strengthened by EPS and CFRP Liner

Kejie Zhai [1, 2], Mingzhe Dang [1], Yi Zhang [1], Qiang Chen [1], Bin Li [1, 2], Niannian Wang [1, 2], Xueming Du [1, 2], Penglu Cui [1*]

[1] *School of Water Conservancy and Transportation, Zhengzhou University, Zhengzhou 450001, China.*

[2] *Yellow River Laboratory (Henan), Zhengzhou 450001, China.*

Received 28 February 2025; Revised 19 May 2025; Accepted 26 May 2025; Published 01 June 2025

Abstract

Prestressed concrete cylinder pipe (PCCP) has been applied in many large-scale hydraulic engineering projects around the world. And the prestressed wire breakage is the most common form of PCCP damage. Traditional carbon fiber reinforced polymer (CFRP) liner techniques fail to fully exploit the tensile performance of CFRP. Therefore, the method of using EPS cushion and CFRP liner to strengthen the PCCP with broken wire is proposed in this study. To clarify the effect of the proposed method, a finite element three-dimensional model is established and validated using experimental data. Subsequently, the effects of EPS thickness, CFRP thickness, and wire breakage ratio on the stress-strain response of the PCCP are analyzed. Based on different failure modes of the pipe, the influence of EPS and CFRP thickness on the internal pressure bearing capacity is discussed. The study reveals that the synergistic action of the EPS cushion can effectively enhance the internal pressure bearing capacity of the PCCP. As the thickness of EPS cushion and CFRP increases, the bearing capacity almost linearly increases. Under the influence of internal pressure, visible cracks first appear in the concrete core, followed by yielding of the steel cylinder, and finally the steel wire stress reaches its ultimate strength.

Keywords: Prestressed Concrete Cylinder Pipe, Wire Breakage; EPS; CFRP Liner; Trenchless.

1. Introduction

Underground pipelines are the urban lifeline and are vital to the healthy development of the city [1-3]. Prestressed concrete cylinder pipe (PCCP) has been widely used in hydraulic engineering [4, 5]. PCCP is composed of concrete, prestressed steel wire, steel cylinders, and mortar. The steel wire in PCCP always breaks due to factors such as corrosion, resulting in a significant decrease in the bearing capacity of PCCP [6-8].

Zarghamee et al. conducted an exhaustive analysis [9-12] on the adhesive efficacy between prestressed wire and mortar coating, employing both experimental techniques and finite element methodologies. Their study delved into the impact of wire spacing and mortar shrinkage on adhesive performance. Furthermore, employing a multi-layer ring model, they scrutinized the mechanical behavior of PCCP under diverse loads, including internal pressure, external pressure, and fluid weight, comparing theoretical calculations with experimental findings. Employing principles of elastic mechanics and finite element analysis, You et al. [13-15] investigated the failure mechanisms of concrete and steel cylinders within PCCP with fractured wire, probing into the bearing capacity alterations induced by longitudinal cracks. Ge & Sinha [16] proposed a model to assess wire prestressing loss and scrutinized various parameters' effects

* Corresponding author: cuipenglu@zzu.edu.cn

http://dx.doi.org/10.28991/CEJ-2025-011-06-06

on PCCP's structural integrity. These insights aid utilities in effectively managing PCCP pipelines with varying bond qualities. Considering the intricate interplay of pipe joints, Hajali et al. [17-19] utilized finite element methods to explore how factors like wire breakage position and quantity affect PCCP's structural performance. Hu et al. [20] conducted comprehensive experiments and finite element analyses to examine PCCP's structural response during wire breakage, evaluating the wire breakage ratio's impact on internal pressure bearing capacity. Cheng et al. [21], employing fiber optic monitoring technology, analyzed strain distributions under internal pressure across diverse materials, investigating PCCP's behavior under elastic and serviceability limit states.

Zhai et al. [22] proposed a non-linear stress reduction model for steel wires, accounting for mortar's bonding force on prestressed wires, substantiating their model through experimentation, and exploring parameters such as pipe diameter, reinforcement ratio, and wire breakage ratio's effects on PCCP performance. Dong et al. [23] compared three-edge bearing test outcomes against calculations derived from an enhanced ANSI/AWWA C304 program, examining calculation methodologies pre- and post-PCCP cracking. Experimental findings revealed tensile stress occurrences at the crown, invert, and springline, with calculated results aligning well with experimental data pre-concrete core cracking. Employing distributed fiber optic sensors utilizing optical frequency domain reflectometry, Li et al. [24, 25] conducted a full-scale experimental investigation on PCCP's mechanical response under internal pressure, emphasizing the potential of distributed sensing technology for structural health monitoring in both new and existing pipeline infrastructures. Li & Feng [26] established a nonlinear finite element model of PCCP, and used the model to study the damage and degradation of in-service PCCP under internal pressure overload. Wang et al. [27] proposed the use of piezoelectric lead zirconate titanate (PZT) technology to monitor PCCP mortar and concrete. Through theoretical analysis and finite element method, the propagation law of Rayleigh waves was confirmed, and the changes in the measured voltage amplitude curve were consistent with the experimental results, verifying the reliability of the proposed method.

PCCP with broken wires needs to be strengthened, and FRP is widely used in structural engineering rehabilitation [28-31]. Lee & Karbhari [32] studied the mechanical behavior of FRP-lined composites under internal and external pressures via pipe section examinations. Their findings underscored the structural efficacy and expeditious nature of FRP liners, offering a cost-efficient alternative to traditional methods of preventive maintenance and repair. Lee & Lee [33] proposed novel design criteria and methodologies for rehabilitating PCCP with FRP, enabling precise determination of optimal FRP layer quantities by evaluating the limit states of deteriorated PCCP. Hu et al. [34, 35] investigated the efficacy of strengthening PCCP with CFRP liners through comprehensive full-scale testing and finite element simulations, analyzing the impact of CFRP layers on concrete, steel wire, and steel cylinders, while also delineating a systematic design process for PCCP repair utilizing CFRP liners. Zhao et al. [36, 37] expounded upon the utilization of prestressed steel strands to fortify PCCP with fractured wires, delving into the methodology's effects on PCCP. Their theoretical derivations culminated in a preliminary design approach capable of determining the area and optimal center spacing of prestressed steel strands considering prestress loss. Zhai et al. [38-41] proposed strengthening PCCP with externally bonded FRP and studied the influence of parameters such as FRP layers and wire breakage ratio on the load-bearing performance of PCCP through experiments and finite element methods, and they analyzed the mechanical behavior of PCCP strengthened by prestressed CFRP subject to secondary load [42].

The aforementioned study has made significant contributions to the service performance and reinforcement repair of PCCP. However, traditional CFRP liner reinforcement methods fail to fully harness the tensile properties of CFRP. Therefore, Zhai et al. [43] proposed the utilization of EPS and CFRP composite liner reinforcement technology, demonstrating its efficacy in strengthening PCCP. Nevertheless, challenges remain regarding EPS and CFRP composite lining reinforcement technology, such as the thickness of EPS material, CFRP, and the effect of wire breakage ratio on pipe load-bearing performance. Thus, this study addresses these deficiencies by establishing a three-dimensional finite element model and evaluating it through experimental data verification. Subsequently, the impact of EPS material thickness, CFRP thickness, and wire breakage ratio on PCCP performance is analyzed. The research findings serve as a reference for the reinforcement of PCCP with broken wires.

2. Finite Element Model

Using ABAQUS, a three-dimensional finite element model is established [44, 45]. Concrete core, mortar coating, and EPS are simulated using three-dimensional solid elements; CFRP and steel cylinder are simulated using shell elements; prestressed steel wires are simulated using three-dimensional truss elements. The prestressed steel wires are embedded in the mortar, the steel cylinder is embedded in the concrete, and bonding is employed between the concrete and mortar. The contact between EPS and the concrete inner wall, as well as CFRP, is simulated using bonding. Concrete and mortar materials are simulated using a concrete damage plastic model; a steel cylinder is simulated using an ideal elastic-plastic model; CFRP is simulated using an ideal elastic-brittle model. The EPS material is simulated by the "Crashable-Foam" model, and the elastic modulus and Poisson's ratio are 2.27 MPa and 0.03, respectively. The geometric dimensions of the model are identical to those in the study by Zhai et al. [43]. The model mesh division is shown in Figure 1.

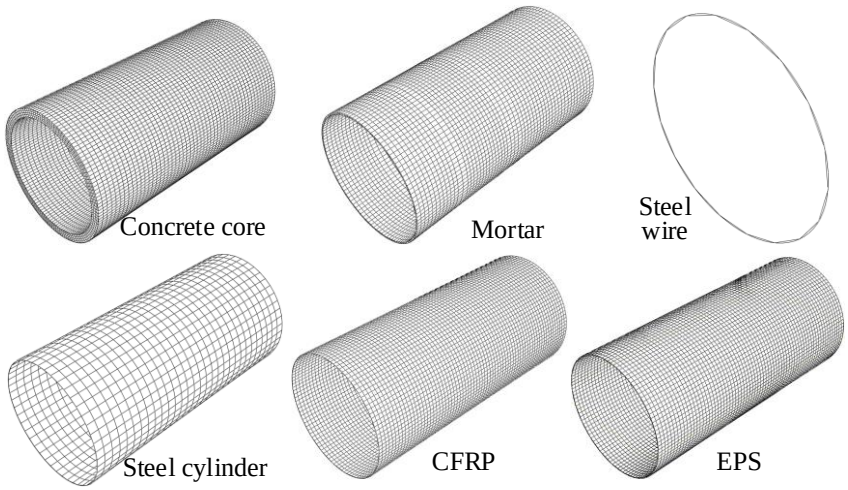

Figure 1. Mesh of the finite element model

Without considering the conditions of wire breakage and repair, utilize the experimental results from reference [46] to evaluate the finite element results, as shown in Figure 2. One can see that the results of the experiment coincide well with the finite element model. Under the internal pressure of 0.7 MPa, the difference in prestressed wire strain between the test and finite element is 7.3%. For concrete core and mortar coating, the maximum difference between the test and model lies between 9.2% and 21.5%, respectively.

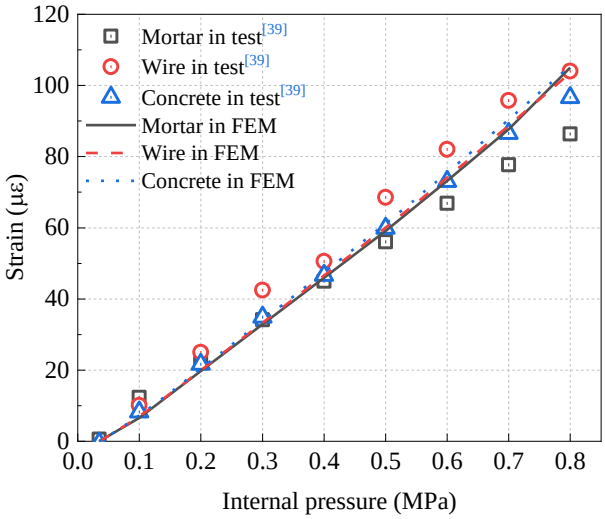

Figure 2. Evaluation of the finite element model

3. Results and Discussion

In this section, the effect of EPS thickness, CFRP thickness, and wire breakage ratio on the mechanical response of PCCP are studied.

3.1. Effect of the EPS Thickness

When considering various thicknesses of EPS, the relationship between internal pressure and maximum principal strain of concrete cores varies, as illustrated in Figure 3. From the figure, it is evident that in the initial stages of increasing internal pressure, the strain of concrete increases linearly with internal pressure, albeit with a small magnitude of increase. At internal pressures of 0.84 MPa, 1.04 MPa, 1.15 MPa, 1.24 MPa, and 1.34 MPa, with EPS thicknesses of 0 mm, 5 mm, 8 mm, 10 mm, and 13 mm, respectively, concrete reaches the strain of micro-cracking, and there is a sharp increase in strain. When the internal pressure reaches 1.03 MPa, 1.23 MPa, 1.35 MPa, 1.44 MPa, and 1.54 MPa, respectively, with different EPS thicknesses, concrete reaches its visible cracking strain, and PCCP reaches its serviceability limit state. Based on the serviceability limit state, the internal pressure bearing capacity of the PCCP strengthened by EPS with thicknesses of 5 mm, 8 mm, 10 mm, and 13 mm will increase by 19.4%, 31.1%, 39.8%, and 49.5%, respectively.

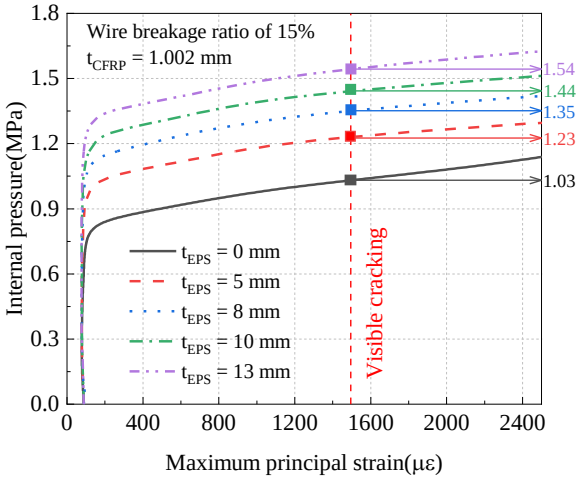

Figure 3. Relationship of internal pressure and concrete strain when different EPS thickness

When different thicknesses of EPS are applied, the damage contour of the concrete core is illustrated in Figure 4. It is evident from the figure that as the thickness of EPS increases, both the extent and area of concrete damage progressively decrease, indicating that the augmentation of EPS thickness contributes to the enhancement of PCCP's load-bearing capacity. It is noteworthy that in Figure 4, the wire breakage ratio of PCCP is 15%, the thickness of CFRP is 1.002 mm, and the internal pressure is 1.5 MPa.

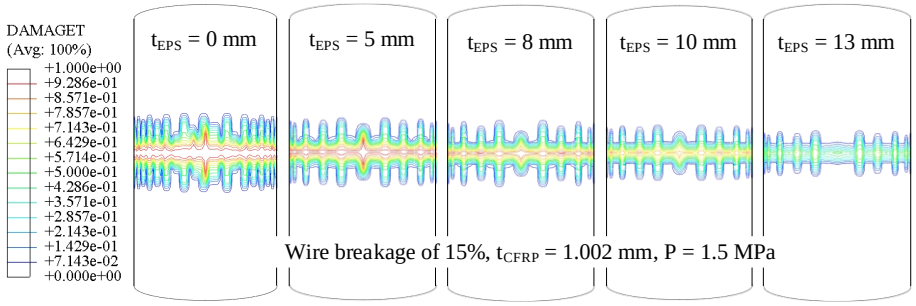

Figure 4. Damage contour of concrete core when different EPS thickness

When varying thicknesses of EPS are employed, the relationship between circumferential stress in the steel cylinder and internal pressure is depicted in Figure 5. As depicted in the figure, during the initial stages of gradual increase in internal pressure, the stress in the steel cylinder also gradually increases. However, a steep rise in steel cylinder stress occurs after the appearance of micro-cracking in the concrete. At internal pressures of 1.36 MPa, 1.51 MPa, 1.66 MPa, 1.76 MPa, and 1.91 MPa, with EPS thicknesses of 0 mm, 5 mm, 8 mm, 10 mm, and 13 mm, respectively, the steel cylinder reaches its yield stress, marking the elastic limit state of the PCCP. Based on the elastic limit state, the internal pressure bearing capacity of the PCCP strengthened by EPS with thicknesses of 5 mm, 8 mm, 10 mm, and 13 mm will increase by 11.0%, 22.1%, 29.4%, and 40.4%, respectively.

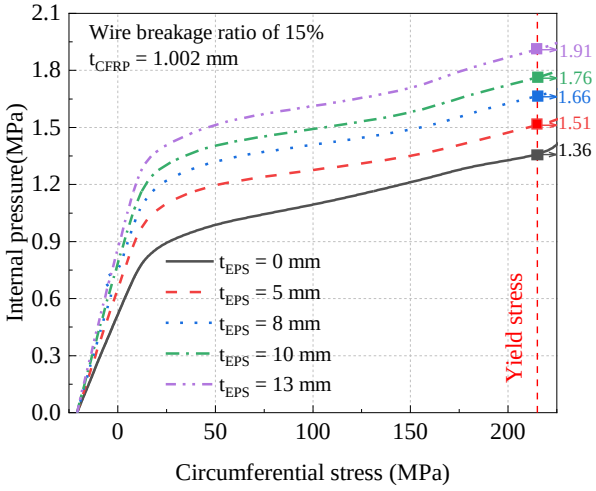

Figure 5. Relationship of internal pressure and cylinder stress when different EPS thickness

When varying thicknesses of EPS are employed, the circumferential stress contour of the steel cylinder is depicted in Figure 6. As illustrated in the figure, with an increase in EPS thickness, the stress in the steel cylinder gradually diminishes, indicating that augmenting the EPS thickness can mitigate the damage to the PCCP. It is noteworthy that in Figure 6, the wire breakage ratio of PCCP is 15%, the thickness of CFRP is 1.002 mm, and the internal pressure is 1.5 MPa.

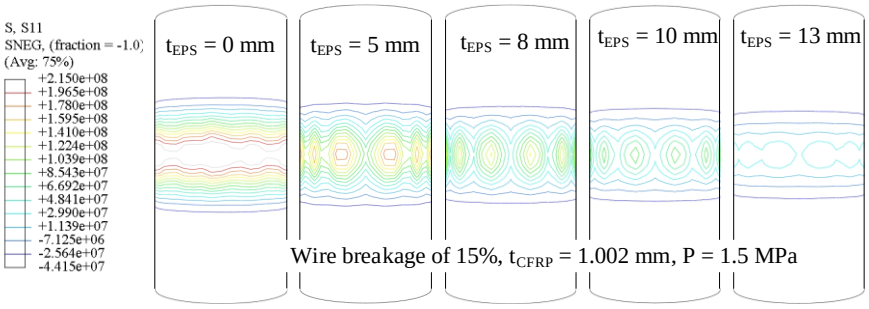

Figure 6. Stress contour of steel cylinder when different EPS thickness

When considering different thicknesses of EPS, the variation in maximum principal stress of CFRP with internal pressure is depicted in Figure 7. The stress in CFRP increases continuously with the rise in internal pressure. Moreover, as the thickness of EPS increases, the stress in CFRP also escalates, indicating that increasing the EPS thickness allows for optimal utilization of CFRP. At an internal pressure of 1.5 MPa, with EPS thicknesses of 0mm, 5mm, 8mm, 10mm, and 13mm, the CFRP stress levels are recorded as 439.56 MPa, 571.89 MPa, 681.09 MPa, 752.34 MPa, and 848.58 MPa, respectively, all of which remain below their ultimate tensile strength.

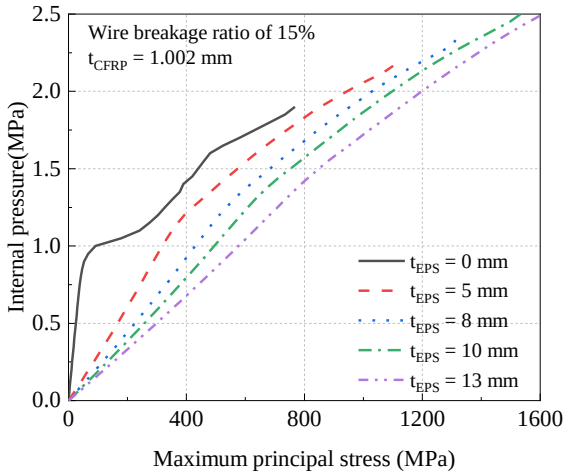

Figure 7. Relationship of internal pressure and CFRP stress when different EPS thickness

When varying thicknesses of EPS are considered, the CFRP stress contour is illustrated in Figure 8. With the increase in EPS thickness, the stress in CFRP progressively escalates, indicating that augmenting the EPS thickness leads to greater internal pressure borne by CFRP, thereby enhancing the internal pressure bearing capacity of PCCP. In Figure 8, the wire breakage ratio of PCCP is 15%, the thickness of CFRP is 1.002 mm, and the internal pressure is 1.5 MPa.

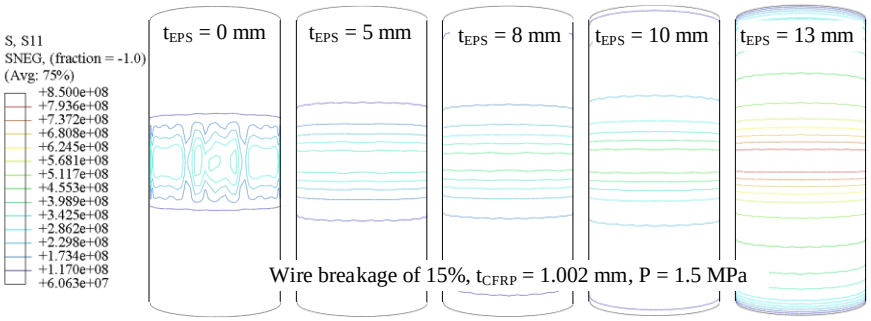

Figure 8. Stress contour of CFRP when different EPS thickness

When considering different thicknesses of EPS, the relationship between wire stress and internal pressure is depicted in Figure 9. With the increase in internal pressure, the stress in the steel wire steadily rises. Conversely, with the increase in EPS thickness, the stress in the steel wire gradually diminishes, reducing the likelihood of PCCP bursting. At EPS thicknesses of 0mm, 5mm, 8mm, 10mm, and 13mm, corresponding to internal pressures of 1.40MPa, 1.61 MPa, 1.76MPa, 1.86MPa, and 2.02MPa, respectively, the steel wire stress reaches 80% of its ultimate strength. Based on 0.8 f_{su}, the internal pressure bearing capacity of the PCCP strengthened by EPS with thicknesses of 5 mm, 8 mm, 10 mm, and 13 mm will increase by 15.0%, 25.7%, 32.9%, and 44.3%, respectively.

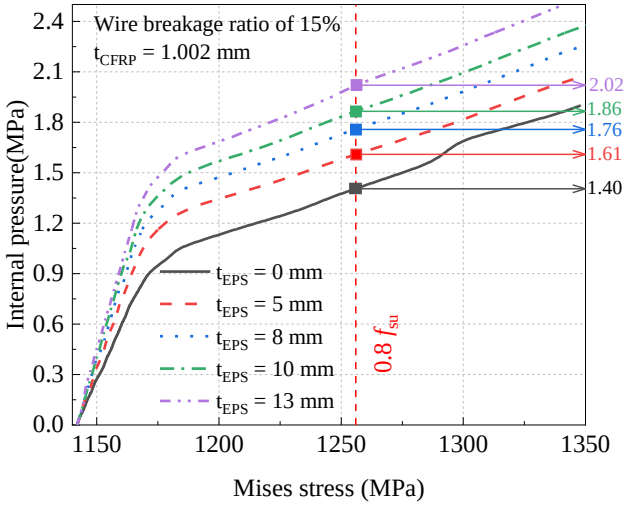

Figure 9. Relationship of internal pressure and wire stress when different EPS thickness

The stress contour of the steel wire is illustrated in Figure 10. Under a pressure of 1.5MPa, the steel wire stress is recorded as 1177.0 MPa, 1187.5 MPa, 1205.8 MPa, 1234.4 MPa, and 1275.2 MPa, for EPS thicknesses of 13 mm, 10 mm, 8 mm, 5 mm, and 0 mm, respectively.

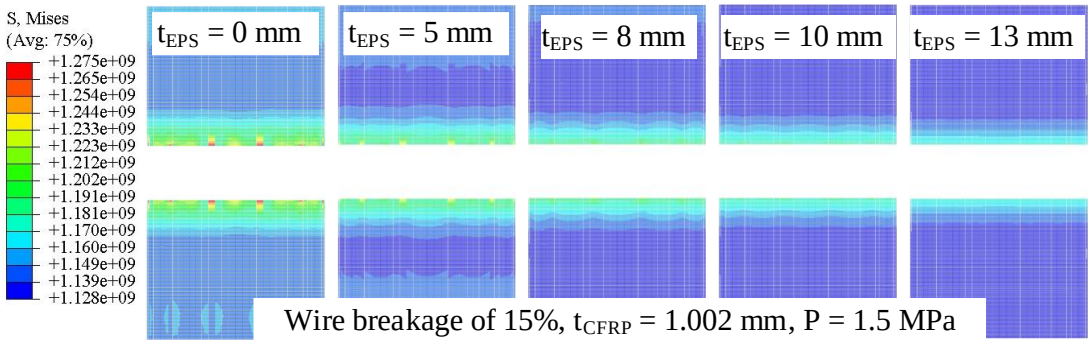

Figure 10. Stress contour of steel wire when different EPS thickness

3.2. Effect of the CFRP Thickness

When considering various thicknesses of CFRP, the relationship between internal pressure and maximum principal strain in the concrete core is depicted in Figure 11. During the initial stages of gradual internal pressure increase, the concrete strain exhibits a linear but slow increase. However, with CFRP layers of 0, 2, 4, 6, and 8, and internal pressures of 0.80 MPa, 0.94 MPa, 1.04 MPa, 1.15 MPa, and 1.25 MPa respectively, micro-cracks appear in the concrete, followed by a steep rise in concrete strain. Visible cracks in the concrete occur at internal pressures of 0.97 MPa, 1.12 MPa, 1.23 MPa, 1.35 MPa, and 1.45 MPa, respectively, marking the PCCP's serviceability limit state. Based on the serviceability limit state, the internal pressure bearing capacity of the PCCP strengthened by CFRP with thicknesses of 2-layer, 4-layer, 6-layer, and 8-layer will increase by 15.5%, 26.8%, 39.2%, and 49.5%, respectively. It should be noted that each layer of CFRP has a thickness of 0.167 mm, with a wire breakage rate of 15% in Figure 11, and an EPS thickness of 8 mm.

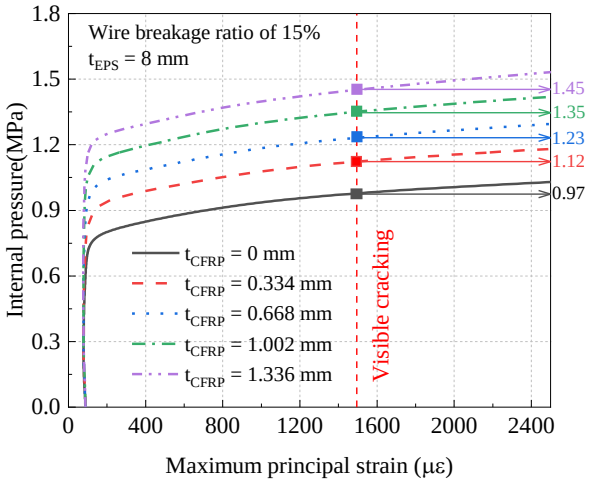

Figure 11. Relationship of internal pressure and concrete strain when different CFRP thickness

When different thicknesses of CFRP are applied, the damage contour of the concrete core is illustrated in Figure 12. It is evident from the figure that as the thickness of CFRP increases, both the extent and area of concrete damage progressively decrease, indicating that the augmentation of CFRP thickness contributes to the enhancement of PCCP's load-bearing capacity.

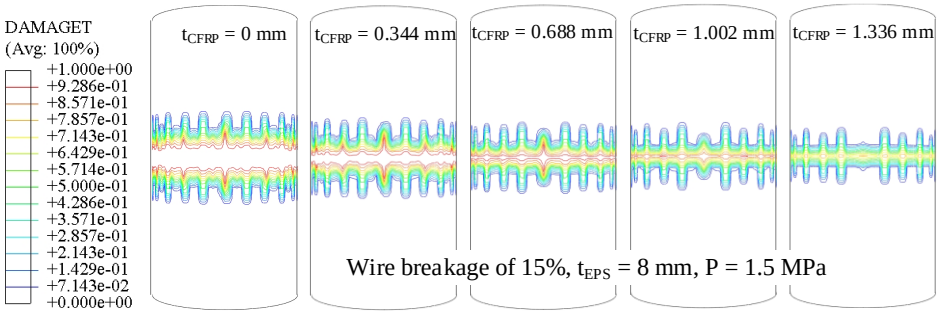

Figure 12. Concrete damage contour when different CFRP thickness

When considering different thicknesses of CFRP, the relationship between circumferential stress in the steel cylinder and internal pressure is illustrated in Figure 13. As depicted in the figure, when the CFRP layers are 0, 2, 4, 6, and 8, the internal pressure reaches 1.16 MPa, 1.33 MPa, 1.50 MPa, 1.66 MPa, and 1.83 MPa respectively, leading the steel cylinder to yield stress, marking the elastic limit state of the PCCP. Based on the elastic limit state, the internal pressure bearing capacity of the PCCP strengthened by CFRP with thicknesses of 2-layer, 4-layer, 6-layer, and 8-layer will increase by 14.7%, 29.3%, 43.1%, and 57.8%, respectively. The stress contour of the steel cylinder is shown in Figure 14. When the CFRP layers are 0, 2, and 4, under an internal pressure of 1.5 MPa, the steel cylinder yields, with the yield area decreasing as the number of CFRP layers increases. At CFRP layer thicknesses of 6 and 8, the steel cylinder stresses are 154.7 MPa and 87.8 MPa, respectively, reaching yield states of 72% and 40.8% respectively.

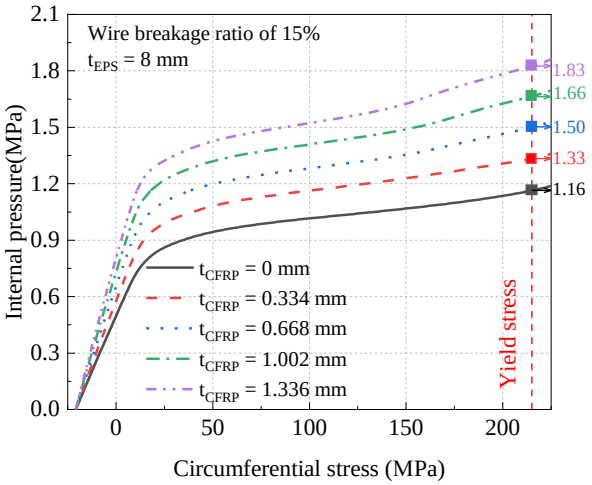

Figure 13. Relationship of internal pressure and cylinder stress when different CFRP thickness

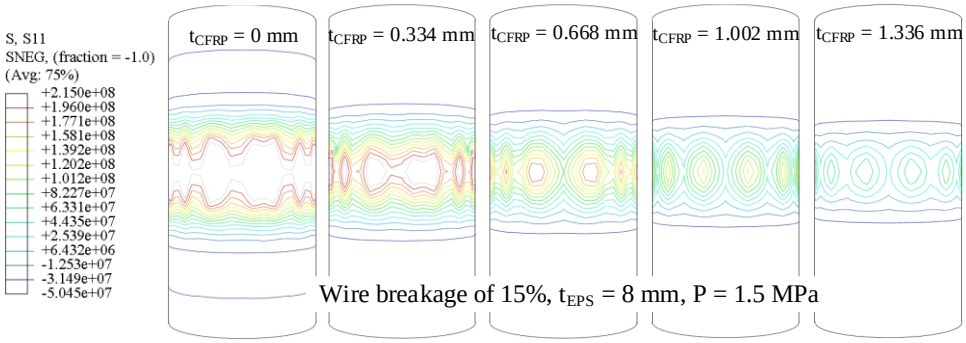

Figure 14. Stress contour of steel cylinder when different CFRP thickness

When considering various thicknesses of CFRP, the relationship between maximum principal stress in CFRP and internal pressure is depicted in Figure 15. CFRP stress increases with the rise in internal pressure and decreases with the increase in CFRP layers, indicating that augmenting CFRP layers contributes to an increase in the load-bearing capacity of PCCP. The stress contour of CFRP is illustrated in Figure 16, where the CFRP stress levels for layer counts of 2, 4, 6, and 8 are 983.8 MPa, 798.4 MPa, 668.6 MPa, and 598.4 MPa respectively, corresponding to 28.9%, 23.5%, 19.7%, and 17.6% of their ultimate strength, respectively.

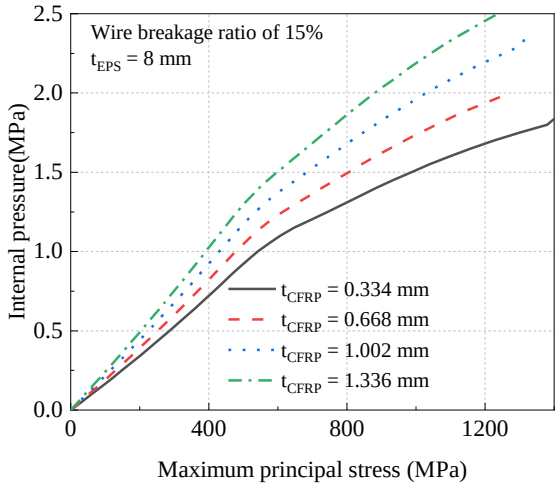

Figure 15. Relationship of internal pressure and CFRP stress when different CFRP thickness

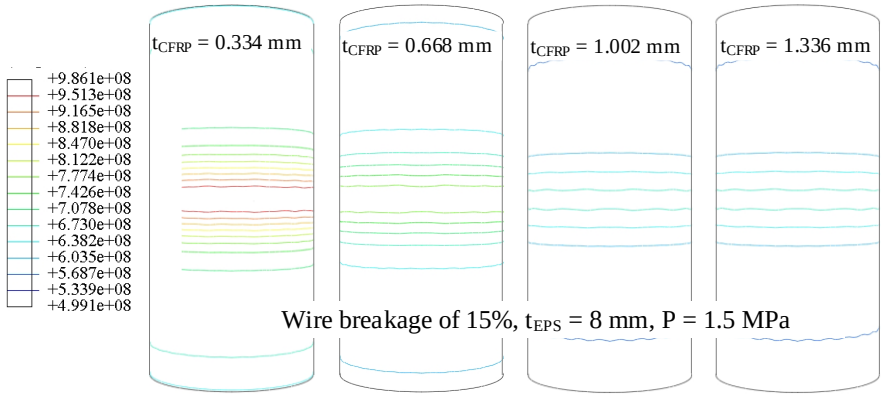

Figure 16. Stress contour of CFRP when different CFRP thickness

When considering different thicknesses of CFRP, the relationship between wire stress and internal pressure is depicted in Figure 17. With the increase in internal pressure, the stress in the steel wire steadily rises. Conversely, with the increase in CFRP thickness, the stress in the steel wire gradually diminishes, reducing the likelihood of PCCP bursting. At CFRP layers of 0, 2, 4, 6, and 8, corresponding to internal pressures of 1.25 MPa, 1.43 MPa, 1.60MPa, 1.76MPa, and 1.94 MPa, respectively, the steel wire stress reaches 80% of its ultimate strength. Based on the state of 0.8 f_{su}, the internal pressure bearing capacity of the PCCP strengthened by CFRP with thicknesses of 2-layer, 4-layer, 6-layer, and 8-layer will increase by 14.4%, 28.0%, 40.8%, and 55.2%, respectively.

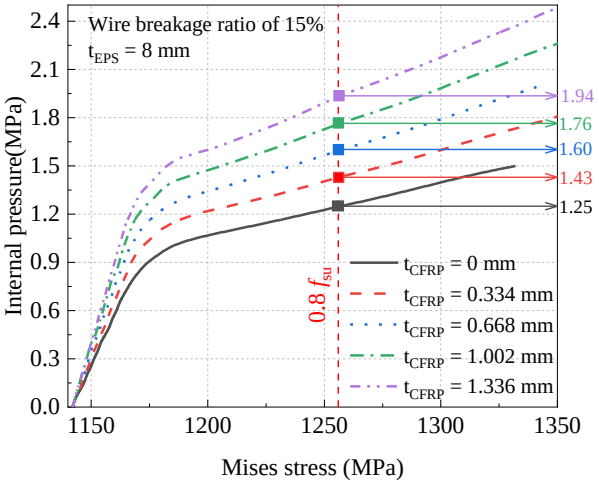

Figure 17. Relationship of internal pressure and wire stress when different CFRP thickness

The stress contour of the steel wire is illustrated in Figure 18. Under a pressure of 1.5MPa, the steel wire stress is recorded as 1131.9 MPa, 1277.5 MPa, 1237.0 MPa, 1206.1 MPa, and 1182.5 MPa, for CFRP layer of 0, 2, 4, 6, and 8, respectively.

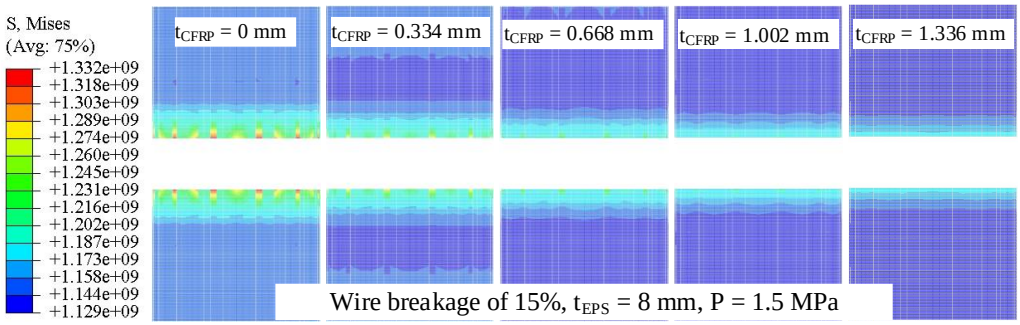

Figure 18. Stress contour of steel wire when different CFRP thickness

3.3. Effect of the Wire Breakage Ratio

When considering different wire breakage ratios, the relationship between maximum principal strain in the concrete core and internal pressure is depicted in Figure 19. When the wire breakage ratio is 5%, a linear relationship between strain and internal pressure is observed at internal pressures ranging from 0 to 2.5 MPa. With wire breakage rates of 10%, 15%, and 20%, during the initial stage of increasing internal pressure, strain exhibits a linear growth trend with internal pressure. Internal pressures reach 2.27 MPa, 1.50 MPa, and 1.10 MPa, respectively, and micro-cracks begin to appear in the concrete, followed by a steep increase in strain. For PCCP with wire breakage ratios of 15% and 20%, visible cracks in the concrete occur when the internal pressure reaches 1.71 MPa and 1.31 MPa respectively, marking the PCCP's service limit state.

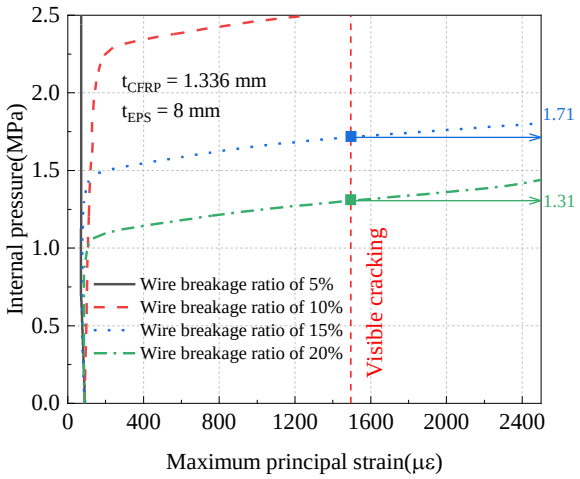

Figure 19. Relationship of internal pressure and concrete strain when different wire breakage ratio

When different wire breakage ratios of PCCP, the damage contour of the concrete core is illustrated in Figure 20. It is evident from the figure that there is almost no damage in concrete when the wire breakage ratio is 5%, as the wire breakage ratio increases, both the extent and area of concrete damage progressively increase.

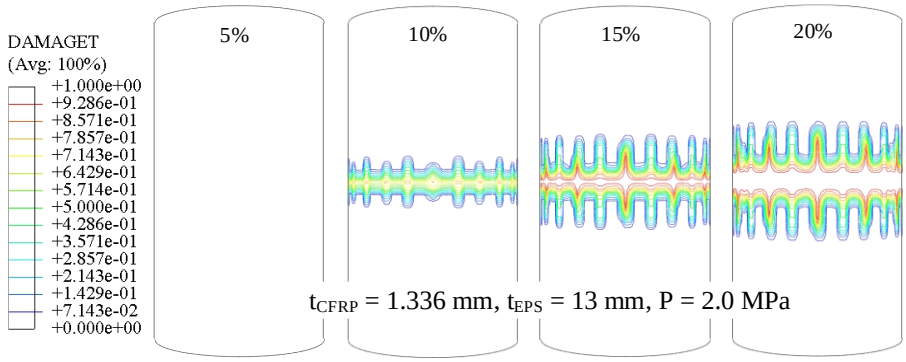

Figure 20. Damage contour of concrete core when different wire breakage ratio

When considering different wire breakage ratios, the relationship between internal pressure and circumferential stress in the steel cylinder is depicted in Figure 21. The stress in the steel cylinder increases with the rise in wire breakage ratio and internal pressure. When the wire breakage ratio is 5%, a linear relationship between stress and pressure is observed within the range of 0 to 2.5 MPa. At wire breakage ratios of 15% and 20%, the steel cylinder stress reaches its yield strength at internal pressures of 2.15 MPa and 1.66 MPa, respectively, marking the elastic limit state of the PCCP.

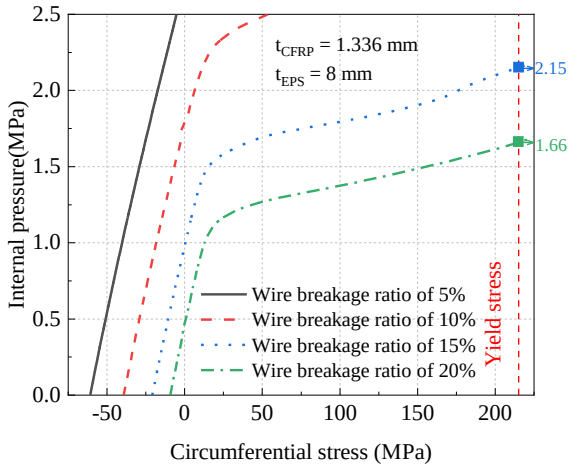

Figure 21. Relationship of internal pressure and cylinder stress when different wire breakage ratio

The stress contour of the steel cylinder is illustrated in Figure 22. Under an internal pressure of 1.5 MPa, when the wire breakage ratios are 5% and 10%, the steel cylinder remains under compression; however, at wire breakage ratios of 15% and 20%, the steel cylinder stress transitions to tensile stress, measured at 15.4 MPa and 155.6 MPa respectively.

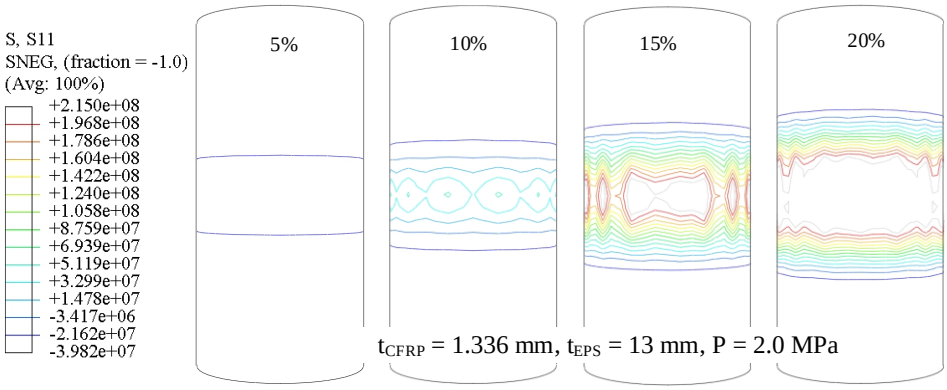

Figure 22. Stress contour of steel cylinder when different wire breakage ratio

When different wire breakage ratios, the relationship between internal pressure and the maximum principal stress of CFRP is illustrated in Figure 23. As depicted in the figure, CFRP stress increases with increasing wire breakage ratio and internal pressure. When the wire breakage ratios are 5% and 10%, the CFRP stress curves essentially overlap,

indicating minimal effectiveness of CFRP at these points. At an internal pressure of 2.0 MPa, wire breakage ratios of 5%, 10%, 15%, and 20% correspond to CFRP stresses of 945.6 MPa, 954.3 MPa, 1021.9 MPa, and 1133.9 MPa, respectively. The CFRP stress contour is depicted in Figure 24.

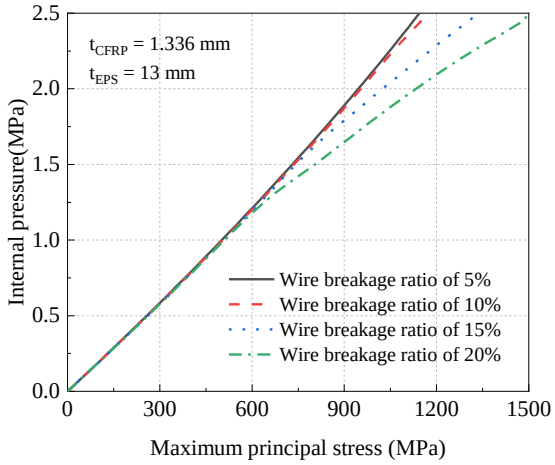

Figure 23. Relationship of internal pressure and CFRP stress when different wire breakage ratio

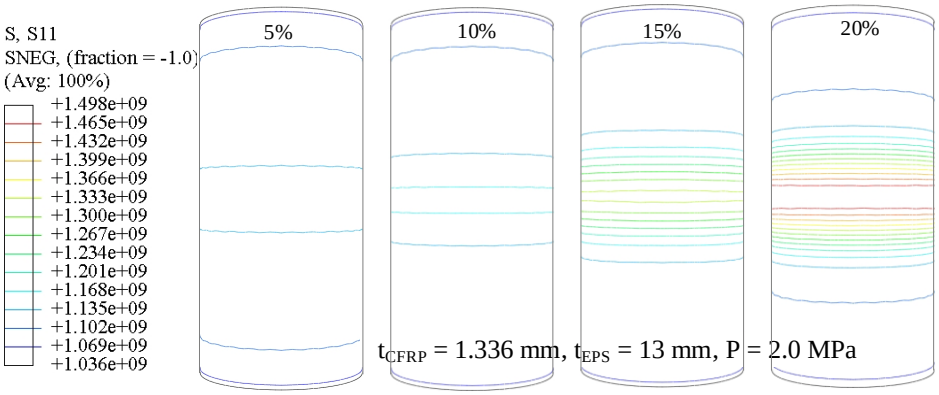

Figure 24. Stress contour of CFRP when different wire breakage ratio

When varying the wire breakage ratio, the relationship between steel wire stress and internal pressure is illustrated in Figure 25. It is evident from the figure that steel wire stress increases with the rise in both wire breakage ratio and internal pressure. When the internal pressures are 2.04 MPa and 2.26 MPa, corresponding to wire breakage ratios of 20% and 15% respectively, the steel wires reach 80% of their ultimate strength. The stress distribution of the steel wires is depicted in the stress contour plot shown in Figure 26. Under an internal pressure of 2.0 MPa, the steel wire stresses in PCCP with wire breakage ratios of 5%, 10%, 15%, and 20% are 1163.1 MPa, 1174.3 MPa, 1218.8 MPa, and 1247.3 MPa respectively.

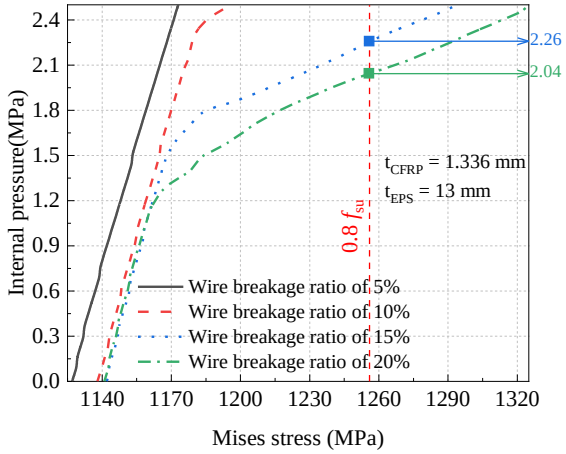

Figure 25. Relationship of internal pressure and wire stress when different wire breakage ratio

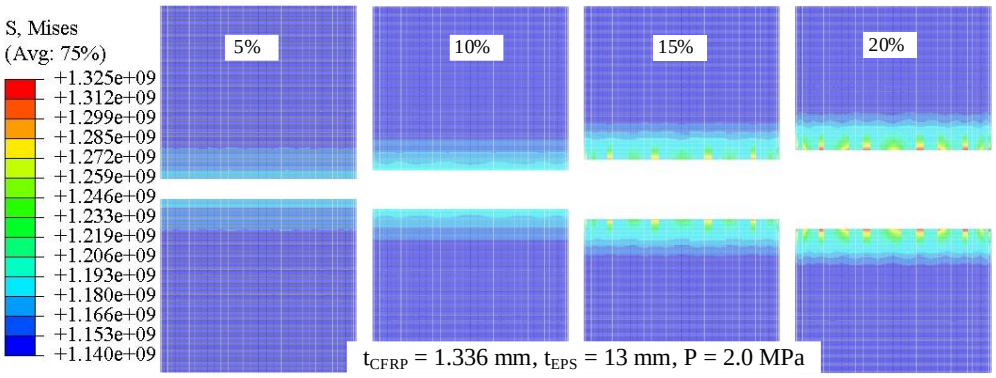

Figure 26. Stress contour of steel wire when different wire breakage ratio

3.4. Discussion

Using the appearance of visible cracks in the concrete core, yielding of the steel cylinder, or when steel wire stress reaches 80% of its ultimate strength as the criteria for determining PCCP failure, the analysis of the variation trend of PCCP bearing capacity with EPS thickness and CFRP thickness is illustrated in Figure 27. As depicted in the figures, under the condition of 15% wire breakage, the internal pressure bearing capacity of PCCP increases almost linearly with the thicknesses of EPS and CFRP. Under the influence of internal pressure, visible cracks first appear in the concrete core, followed by yielding of the steel cylinder, and finally the steel wire stress reaches 80% of its ultimate strength. With 6 layers of CFRP, when visible cracks appear in the concrete core, yielding of the steel cylinder, or when steel wire stress reaches 80% of its ultimate strength, the pipeline bearing capacity is 1.5 MPa for EPS thicknesses of 11.8 mm, 4.35 mm, and 2.38 mm respectively. For an EPS thickness of 8 mm, the pipe bearing capacity is 1.4 MPa for CFRP thicknesses of 7.02×0.167 mm, 2.81×0.167 mm, and 1.68×0.167 mm respectively.

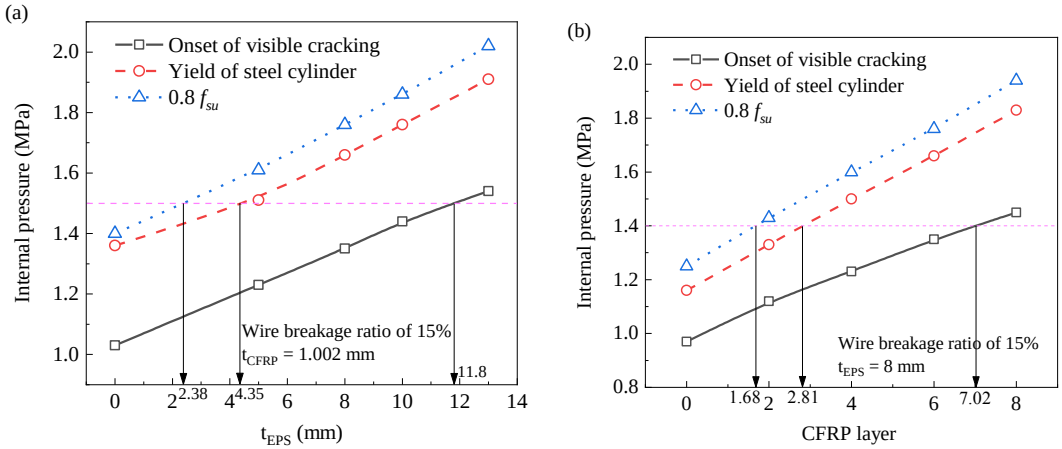

Figure 27. The strength of PCCP varies with changes in the thickness of: (a) EPS and (b) CFRP

4. Conclusion

The CFRP liner reinforcement for PCCP with broken wires can to some extent increase the internal pressure bearing capacity of the PCCP, which has already formed standard specifications in North America. However, the tensile performance of CFRP is not fully utilized. The EPS and CFRP liner reinforcement technology in this study can fully exploit the tensile performance of CFRP, resulting in a significant increase in the bearing capacity of PCCP when using the same thickness of CFRP. Furthermore, this study investigates the effects of EPS thickness, CFRP thickness, and wire breakage ratio on the stress-strain of various materials (such as concrete pipe core, steel cylinder, steel wire), presenting the mechanical response of PCCP from multiple perspectives when reinforced with EPS and CFRP liner. The study found that based on the serviceability limit state, the internal pressure bearing capacity of the PCCP strengthened by EPS with thicknesses of 5 mm, 8 mm, 10 mm, and 13 mm will increase by 19.4%, 31.1%, 39.8%, and 49.5%, respectively. Based on the elastic limit state, the internal pressure bearing capacity will increase by 11.0%, 22.1%, 29.4%, and 40.4%, respectively, indicating that the increase in EPS thickness can significantly increase the internal pressure bearing capacity of the PCCP. In addition, onset of visible crack of concrete core, the pipeline bearing capacity is the lowest, and onset of the state of 0.8 f_{su}, the bearing capacity is the highest.

The reinforcement technology in this paper has significant advantages in terms of mechanical response, but also faces some challenges in reality, such as the reduction of the pipe's flow area, and the bonding performance of EPS with concrete and CFRP. These issues will be gradually addressed in future research.

5. Declarations

5.1. Author Contributions

Conceptualization, X.D.; methodology, K.Z., M.D., Q.C., Y.Z., N.W., and P.C.; software, K.Z., M.D., Q.C., Y.Z., N.W., and P.C.; formal analysis, K.Z.; investigation, K.Z.; resources, X.D. and P.C.; data curation, K.Z.; writing—original draft preparation, K.Z.; project administration, B.L.; funding acquisition, B.L. All authors have read and agreed to the published version of the manuscript.

5.2. Data Availability Statement

The data presented in this study are available in the article.

5.3. Funding

This work was supported by the National Natural Science Foundation of China (52309174), the Natural Science Foundation of Henan (252300421308); the National Postdoctoral Program for Innovative Talents (BX20230328), the China Postdoctoral Science Foundation (2023M743219).

5.4. Conflicts of Interest

The authors declare no conflict of interest.

5.5. Declaration of Competing Interest

The authors declare that there are no conflicts of interest regarding the publication of this paper.

6. References

[1] Koike, T. (2023). Historical aspects of lifeline earthquake engineering. Urban Lifeline, 1(1), 3. doi:10.1007/s44285-023-00004-x.

[2] Rahardjo, H., Zhai, Q., Satyanaga, A., Li, Y., Rangarajan, S., & Rahimi, A. (2023). Slope susceptibility map for preventive measures against rainfall-induced slope failure. Urban Lifeline, 1(1), 5. doi:10.1007/s44285-023-00006-9.

[3] Shaba, A. F., & Masheka, G. (2024). Evaluation of geosynthetic encased columns in Zambian heterogenous soils. Urban Lifeline, 2(1), 5. doi:10.1007/s44285-024-00015-2.

[4] Zhang, P., Yang, J., Zhang, Q., Chen Z., & Zhang, Q. (2022). Key technologies for broken wire of large diameter PCCP, Water Resources and Hydropower Engineering, 53(S2), 120-124. doi:10.13928/j.cnki.wrahe.2022.S2.028.

[5] Liu, Y., Yang, Y., & Yang J. (2021). Research and application of large PCCP water supply pipeline maintenance construction technology, Water Resources and Hydropower Engineering, 52(S1), 223–228. doi:10.13928/j.cnki.wrahe.2021.S1.042.

[6] Huang, Z. & Wang, R. (2021). Finite element analysis investigation of cracks impact on structurual safety performance of PCCP, Water Resources and Hydropower Engineering, 552(4), 88-94. doi:10.13928/j.cnki.wrahe.2021.04.009.

[7] Dong, X., Dou, T., Zhao, L., Cheng, B., & Liu J. (2020). An overview on safety assessment of pre-stressed concrete cylinder pipe (PCCP. Water Resources and Hydropower Engineering, 51(10), 72–80. doi:10.13928/j.cnki.wrahe.2020.10.009.

[8] Zhang, Q. (2019). PCCP reinforcement with prestressing technology, Water Resources and Hydropower Engineering, 50(S1), 126-132. doi:10.13928/j.cnki.wrahe.2019.S1.023.

[9] Zarghamee, M. S., Eggers, D. W., Ojdrovic, R., & Rose, B. (2003). Risk Analysis of Prestressed Concrete Cylinder Pipe with Broken Wires. New Pipeline Technologies, Security, and Safety, 599–609. doi:10.1061/40690(2003)81.

[10] Zarghamee, M. S., & Fok, K. (1990). Analysis of Prestressed Concrete Pipe under Combined Loads. Journal of Structural Engineering, 116(7), 2022–2039. doi:10.1061/(asce)0733-9445(1990)116:7(2022).

[11] Zarghamee, M. S., Ojdrovic, R. P., & Dana, W. R. (1993). Coating Delamination by Radial Tension in Prestressed Concrete Pipe. II: Analysis. Journal of Structural Engineering, 119(9), 2720–2732. doi:10.1061/(asce)0733-9445(1993)119:9(2720).

[12] Zarghamee, M. S., Ojdrovic, R. P., & Dana, W. R. (1993). Coating Delamination by Radial Tension in Prestressed Concrete Pipe. I: Experiments. Journal of Structural Engineering, 119(9), 2701–2719. doi:10.1061/(asce)0733-9445(1993)119:9(2701).

[13] You, R. (2012). Longitudinal Cracking Analysis of PCCP with Broken Wires. Applied Mechanics and Materials, 157–158, 976–981. doi:10.4028/www.scientific.net/amm.157-158.976.

[14] You, R., & Gong, H. (2012). Failure analysis of PCCP with broken wires. Applied Mechanics and Materials, 193–194, 855–858. doi:10.4028/www.scientific.net/AMM.193-194.855.

[15] You, R., & Gong, H. (2012). Steel-cylinder yielding analysis of PCCP with broken wires. Advanced Materials Research, 503–504, 819–823. doi:10.4028/www.scientific.net/AMR.503-504.819.

[16] Ge, S., & Sinha, S. (2015). Effect of Mortar Coating's Bond Quality on the Structural Integrity of Prestressed Concrete Cylinder Pipe with Broken Wires. Journal of Materials Science Research, 4(3), 59–75. doi:10.5539/jmsr.v4n3p59.

[17] Hajali, M., Alavinasab, A., & Shdid, C. A. (2015). Effect of the location of broken wire wraps on the failure pressure of prestressed concrete cylinder pipes. Structural Concrete, 16(2), 297–303. doi:10.1002/suco.201400070.

[18] Hajali, M., Alavinasab, A., & Abi Shdid, C. (2016). Structural performance of buried prestressed concrete cylinder pipes with harnessed joints interaction using numerical modeling. Tunnelling and Underground Space Technology, 51, 11–19. doi:10.1016/j.tust.2015.10.016.

[19] Hajali, M., Alavinasab, A., & Shdid, C. A. (2016). Effect of the Number of Broken Wire Wraps on the Structural Performance of PCCP with Full Interaction at the Gasket Joint. Journal of Pipeline Systems Engineering and Practice, 7(2), 1–8. doi:10.1061/(asce)ps.1949-1204.0000219.

[20] Hu, B., Fang, H., Wang, F., & Zhai, K. (2019). Full-scale test and numerical simulation study on load-carrying capacity of prestressed concrete cylinder pipe (PCCP) with broken wires under internal water pressure. Engineering Failure Analysis, 104, 513–530. doi:10.1016/j.engfailanal.2019.06.049.

[21] Cheng, B., Dou, T., Xia, S., Zhao, L., Yang, J., & Zhang, Q. (2020). Mechanical properties and loading response of prestressed concrete cylinder pipes under internal water pressure. Engineering Structures, 216, 1–11. doi:10.1016/j.engstruct.2020.110674.

[22] Zhai, K., Guo, C., Fang, H., Li, B., Ma, B., Hu, Q., & Wang, F. (2021). Stress distribution and mechanical response of PCCP with broken wires. Engineering Structures, 245, 245. doi:10.1016/j.engstruct.2021.112858.

[23] Dong, X., Dou, T., Dong, P., Wang, Z., Li, Y., Ning, J., Wei, J., Li, K., & Cheng, B. (2022). Failure experiment and calculation model for prestressed concrete cylinder pipe under three-edge bearing test using distributed fiber optic sensors. Tunnelling and Underground Space Technology, 129, 129. doi:10.1016/j.tust.2022.104682.

[24] Li, K., Li, Y., Dong, P., Wang, Z., Dou, T., Ning, J., Dong, X., & Si, Z. (2022). Pressure test of a prestressed concrete cylinder pipe using distributed fiber optic sensors: Instrumentation and results. Engineering Structures, 270, 114835. doi:10.1016/j.engstruct.2022.114835.

[25] Li, K., Li, Y., Dong, P., Wang, Z., Dou, T., Ning, J., Dong, X., Si, Z., & Wang, J. (2022). Mechanical properties of prestressed concrete cylinder pipe with broken wires using distributed fiber optic sensors. Engineering Failure Analysis, 141, 106635. doi:10.1016/j.engfailanal.2022.106635.

[26] Li, H., & Feng, X. (2025). Numerical investigations into the damage mechanism and failure mode of large-scale PCCPs under internal pressure overload. Structural Concrete. doi:10.1002/suco.70044.

[27] Wang, X., Hu, S., Li, W., & Hu, Y. (2025). Rayleigh wave-based monitoring of mortar coating and concrete core cracking on prestressed concrete cylinder pipe under external pressure using piezoelectric lead zirconate titanate. Tunnelling and Underground Space Technology, 155, 155. doi:10.1016/j.tust.2024.106220.

[28] Deng, Z., & Liu, S. (2016). Test and modeling of ultra-high performance concrete confined by fiber reinforced polymer tube. Journal of Basic Science and Engineering, 24(4), 792–803. doi:10.16058/j.issn.1005-0930.2016.04.015.

[29] Lu, Y., Huang, Y., Liu, Z., & Wang, X. (2022). Research on Masonry Columns Strengthened with the Combination of Angle Steel and GFRP Under Axial Load. Yingyong Jichu Yu Gongcheng Kexue Xuebao/Journal of Basic Science and Engineering, 30(3), 645–656. doi:10.16058/j.issn.1005-0930.2022.03.011.

[30] Xu, J., Chen, W., Huang, X., Chen, Z., & Tan, C. (2022). Calculation Approach of Ultimate Compressive Strain in FRP-Confined Concrete Based on Bayesian Modification. Yingyong Jichu Yu Gongcheng Kexue Xuebao/Journal of Basic Science and Engineering, 30(4), 974–986. doi:10.16058/j.issn.1005-0930.2022.04.015.

[31] Pandey, A. K. P. K., Dada, M., Patton, M. L., & Adak, D. (2024). A comparative review on the structural behaviour of GFRP rebars with conventional steel rebars in reinforced concrete columns. Innovative Infrastructure Solutions, 9(10), 373. doi:10.1007/s41062-024-01686-0.

[32] Lee, D. C., & Karbhari, V. M. (2005). Rehabilitation of large diameter prestressed cylinder concrete pipe (PCCP) with FRP composites - Experimental investigation. Advances in Structural Engineering, 8(1), 31–44. doi:10.1260/1369433053749634.

[33] Lee, Y., & Lee, E. T. (2013). Retrofit Design of Damaged Prestressed Concrete Cylinder Pipes. International Journal of Concrete Structures and Materials, 7(4), 265–271. doi:10.1007/s40069-013-0057-9.

[34] Hu, H., Niu, F., Dou, T., & Zhang, H. (2018). Rehabilitation effect evaluation of CFRP-lined prestressed concrete cylinder pipe under combined loads using numerical simulation. Mathematical Problems in Engineering, 2018, 1–17. doi:10.1155/2018/3268962.

[35] Hu, H., Dou, T., Niu, F., Zhang, H., & Su, W. (2019). Experimental and numerical study on CFRP-lined prestressed concrete cylinder pipe under internal pressure. Engineering Structures, 190, 480–492. doi:10.1016/j.engstruct.2019.03.106.

[36] Zhao, L., Dou, T., Cheng, B., Xia, S., Yang, J., Zhang, Q., Li, M., & Li, X. (2019). Experimental study on the reinforcement of prestressed concrete cylinder pipes with external prestressed steel strands. Applied Sciences (Switzerland), 9(1), 1–19. doi:10.3390/app9010149.

[37] Zhao, L., Dou, T., Cheng, B., Xia, S., Yang, J., Zhang, Q., Li, M., & Li, X. (2019). Theoretical study and application of the reinforcement of prestressed concrete cylinder pipes with external prestressed steel strands. Applied Sciences (Switzerland), 9(24), 5532. doi:10.3390/app9245532.

[38] Zhai, K., Fang, H., Guo, C., Ni, P., Fu, B., Wang, F., & Zhang, C. (2021). Strengthening of PCCP with broken wires using prestressed CFRP. Construction and Building Materials, 267, 120903. doi:10.1016/j.conbuildmat.2020.120903.

[39] Zhai, K., Fang, H., Guo, C., Ni, P., Wu, H., & Wang, F. (2021). Full-scale experiment and numerical simulation of prestressed concrete cylinder pipe with broken wires strengthened by prestressed CFRP. Tunnelling and Underground Space Technology, 115, 104021. doi:10.1016/j.tust.2021.104021.

[40] Zhai, K., Fang, H., Li, B., Guo, C., Yang, K., Du, X., Du, M., & Wang, N. (2023). Failure experiment on CFRP-strengthened prestressed concrete cylinder pipe with broken wires. Tunnelling and Underground Space Technology, 135, 105032. doi:10.1016/j.tust.2023.105032.

[41] Zhai, K., Fang, H., Yang, M., Sun, M., Zhang, X., Zhao, X., Xue, B., Lei, J., & Yao, X. (2023). The impacts of CFRP widths and thicknesses on the strengthening of PCCP. Structures, 56, 104856. doi:10.1016/j.istruc.2023.07.046.

[42] Hu, H., Dou, T., Niu, F., Zhang, H., & Su, W. (2019). Experimental and numerical study on CFRP-lined prestressed concrete cylinder pipe under internal pressure. Engineering Structures, 190, 480-492. doi:10.1016/j.engstruct.2019.03.106.

[43] Zhai, K., Fang, H., Guo, C., Li, B., Wang, N., Yang, K., Zhang, X., Du, X., & Di, D. (2024). Using EPS and CFRP liner to strengthen prestressed concrete cylinder pipe. Construction and Building Materials, 412, 134860. doi:10.1016/j.conbuildmat.2024.134860.

[44] Spring, D. W., & Paulino, G. H. (2014). A growing library of three-dimensional cohesive elements for use in ABAQUS. Engineering Fracture Mechanics, 126, 190-216. doi:10.1016/j.engfracmech.2014.04.004.

[45] Wang, G. D., & Melly, S. K. (2018). Three-dimensional finite element modeling of drilling CFRP composites using Abaqus/CAE: a review. The International Journal of Advanced Manufacturing Technology, 94, 599-614. doi:10.1007/s00170-017-0754-7.

[46] Zhai, K., Fang, H., Guo, C., Fu, B., Ni, P., Ma, H., He, H., & Wang, F. (2021). Mechanical properties of CFRP-strengthened prestressed concrete cylinder pipe based on multi-field coupling. Thin-Walled Structures, 162, 107629. doi:10.1016/j.tws.2021.107629.